

Synthesis of nano-structured sphene and optimization of the mechanical properties of its scaffold via response surface methodology

Amirmostafa Amirjania¹, Masoud Hafezib^{2*}, Ali Zamanianb², Mana Yasaeecc³, Noor Azuan Abu Osmand⁴

¹ Department of Mining and Metallurgical Engineering, Amirkabir University of Technology, Tehran, Iran

² Nanotechnology and Advanced Materials Department, Materials and Energy Research Center, Alborz, Iran

³ Department of Life Science Engineering, Faculty of New Sciences and Technologies, University of Tehran, Tehran, Iran

⁴ Department of Biomedical Engineering, Faculty of Engineering, University of Malaya, Kuala Lumpur, Malaysia

ARTICLE INFO

Article history:

Received 4 February 2016

Accepted 14 July 2016

Available online 15 July 2016

Keywords:

Bioceramics

Mechano-chemical synthesis

Mechanical properties

Response Surface

Methodology

ABSTRACT

Nano-structured sphene (CaTiSiO₅) powder was synthesized via mechanical activation and heat treatment. The synthesized powder was characterized by X-ray diffraction (XRD) analysis, transmission electron microscopy (TEM), and simultaneous thermal analysis (STA). The sphene scaffolds were then fabricated via porogen method (using citric acid). Response surface methodology was used to determine the effects of *d* (particle size) and %V porogen (volume percent of porogen) on the mechanical behavior of the prepared sphene scaffolds. Moreover, a suitable mathematical model for describing the relationship between the factors (*d* and %V porogen) and the response (compressive strength) was statistically developed. The use of porogen in the synthesis procedure can change the porosity value of the final scaffold; thus, the compressive strength of the sphene scaffolds varied widely. The statistical analysis results predicted that the maximum value of the compressive strength can be obtained if %V = 25% and *d* = 250 μm. Under these conditions, the prepared scaffolds possess a compressive strength value as high as 7 MPa.

1. Introduction

Sphene [CaTiSiO₅ or CaTiO(SiO₄)] or titanite is an orthosilicate mineral with monoclinic symmetry [1]. The structural ability of sphene for hosting different cation and anion substitutions has made it a promising material for a wide range of applications [2-4]. Recently, sphene has attracted the attention of biomedical engineers not only for its hosting ability but also because of its high chemical stability and cytocompatibility [5, 6]. Ramaswamy et al. [7]

prepared sphene ceramic coatings for implants. According to the *in vitro* studies, the sphene coatings can support bone formation around the implants by recruiting osteogenic cells and thus enhance osseointegration. Wu et al. [8] performed sphene coating on a titanium alloy (Ti-6Al-4V) via the plasma spray method. The formed sphene coating possesses excellent chemical stability, bonding strength, and cellular bioactivity. To the best of our knowledge, only a few studies have reported on

* Corresponding Author:

Email Address: mhafezi@merc.ac.ir

the biomedical applications of sphene ceramics, and there is a lack of information regarding the effect of pertinent factors in the synthesis of sphene. Previous reports on the synthesis of sphene ceramics were mainly limited to the sol-gel, spray pyrolysis, combustion, coprecipitation, and freeze-drying methods [1, 5, 6, 8]. The formation of other phases, such as cristobalite and perovskite, was the main drawback of the abovementioned methods. Mechanical alloying has been proven to be a promising method for fabricating different ceramic-based biomaterials [1, 9].

Mechanochemical reactions possess advantages such as simplicity, scale up possibility, and low working temperature. Reports on the effect of significant factors in synthesizing sphene powder via mechanical activation are limited [1, 9]. The effects of the factors in all the above mentioned studies were evaluated by investigating one factor at a time. This approach is inefficient for optimization purposes and also gives no complete information about the possible interactions between the factors in a process. An interaction may exist between effective factors in this synthesis process (the optimum factor level may be influenced by the level of the other factors). A factorial design of experiments (DOE) is a method that can simultaneously consider several factors at different levels and provide a proper mathematical model for the relationships between factors and the response via response surface methodology (RSM) [10]. Factorial DOE has been widely used for optimization purposes in different kinds of systems [11-13]. In this work, we conducted mechanical activation and heat treatment for the synthesis of sphene powder in a planetary ball mill. Sphene scaffolds were then fabricated via the purging method. The effects of two main factors, including particle diameter and %V of porogen, on the mechanical behavior of the prepared scaffolds were studied via RSM. A half fractional factorial, central composite design (CCD), was chosen as the matrix of the design to properly identify the probable interaction between two factors as well as to provide a second-order polynomial equation for predicting the optimum level of factors.

2. Experimental procedure

2.1. Synthesis of sphene powder and manufacturing of the scaffold

Appropriate amounts of silica gel, titania, and calcium oxide were mixed to adjust the Ca:Si:Ti molar ratio to 1:1:1. All the materials were in analytical grades and used without further purifications. The powder mixture was milled in a planetary ball mill for 1 h with 300 rpm. A ball to powder ratio of 10 to 1 was considered and the balls (15 mm in diameter) and vials (45 ml capacity) were made of stainless steel. The mass of the balls and the powder was 13.56 gr (for a single ball) and 5 gr, respectively.

The synthesized powders were characterized via simultaneous thermal analysis (STA), X-ray diffraction (XRD) analysis, and transmission electron microscopy (TEM). The milled powders were then calcinated at 900 °C for 3 h at a heating rate of 1 °C /min to form the sphene phase. Different particle sizes of the synthesized powders and various %V of porogen (citric acid as the porogen agent) were used to manufacture the scaffolds. The sphene-sieved powder with different particle sizes (100, 200, and 300 µm) was then mixed with citric acid at 80:20, 65:35, and 50:50 (in V/V). The mixture was isostatically pressed in a steel die under 120 MPa. The specimens were sintered at 900 °C for 1 h.

2.2. Powder characterization

2.2.1. X-Ray Diffraction analysis

Phase analysis was performed using an X-ray diffractometer (model PW3710; Philips) which was operated at the voltage and current settings of 40 kV and 30 mA, respectively. A Cu-K α radiation was also used (1.54 Å). For qualitative analysis, XRD diagrams were recorded in the interval 0° to 80° at a scan speed of 2°/s.

2.2.2. Simultaneous Thermal Analyses

Thermal analyses, such as thermogravimetry (TG) and differential thermal analysis (DTA), were performed on the powder to evaluate the thermal behavior of the sphene powder. These analyses were carried out using a thermo-analyzer (model STA409PC/PG; Netzsch, Germany) operated in the ambient to 1200°C temperature range with a heating rate of 10°C/min.

2.2.3. Transmission Electron Microscopy

Transmission electron microscopy (model GM200 PEG; Philips, Netherlands) was used to observe the morphology of the sphere at 200 kV. The particles were deposited on Cu grids, which support a carbon film via deposition from a dilute suspension in ethanol.

2.2.4. The compressive strength test

The compressive strength of the scaffolds was determined by performing uniaxial tests on the cylindrical-shaped samples by using an apparatus with a cross head speed of 1 mm/min (model STM-20; Santam, Iran). The Young modulus (E), ultimate compressive stress (σ), and toughness data were directly calculated using the device. A minimum of four samples was tested under each testing condition.

2.2.5. Design of the experiments

Design of the experiments for f factors consisted of (1) N_0 experiments in order to obtain pure experimental error of the design in which all of the factors are in their medium levels; (2) $2f$ star points in which all the parameters are in their medium levels except one factor that is set to $-$ or $+$ (In this CCD design was set to 1); (3) and finally $2f$ factorial points. In summary, this design consisted of eleven experimental runs

involving 2 factors and 3 levels. In order to evaluate the model coefficient of the studied factors that are speculated to influence the mechanical properties of the prepared sphere scaffolds, MINITAB Release 15 was used to employ a CCD with multiple linear regression and develop a second-order polynomial mathematical model.

Each factor has three levels and was set at its highest (+1), lowest (-1) and medium levels (0). The design involved two factors, including the particle size and the %V of porogen, and the response is the compressive strength of the prepared scaffold. The levels used for these two factors according to central design and their responses are presented in Tables 1 and 2, respectively.

Appropriate amounts of silica gel, titania, and calcium oxide were mixed to adjust the Ca:Si:Ti molar ratio to 1:1:1. All the materials were in analytical grades and used without further purifications. The powder mixture was milled in a planetary ball mill for 1 h with 300 rpm. A ball to powder ratio of 10 to 1 was considered and the balls (15 mm in diameter) and vials (45 ml capacity) were made of stainless steel. The mass of the balls and the powder was 13.56 gr (for a single ball) and 5 gr, respectively.

Table 1. Experimental ranges for the level of independent variables in response surface study.

Factors	Unit	Notation	Level		
			-1	0	+1
Particle size	μm	d	100	200	300
%V porogen	-	%V	20	35	50

Table 2. Experimental design and results of the central composite design.

Run	Variables		Response
	Particle diameter (μ)	%V Porogen	Compressive strength (MPa)
1	100	20	6.00
2	100	50	0.98
3	300	20	6.73
4	300	50	1.35
5	200	20	5.56
6	200	50	0.74
7	100	35	2.90
8	300	35	3.78
9	200	35	1.37
10	200	35	1.38
11	200	35	1.39

In order to minimize systematic bias, all the experiments were replicated for at least three times and the reported result of each response is the mean value of the obtained responses.

Eq. (1) is the quadratic polynomial regression model employed for estimating and predicting the response value:

$$Y = b_0 + \sum_{i=1}^2 b_i X_i + \sum_{i=1}^2 b_{ii} X_i^2 + \sum_{i=1}^2 \sum_{j=i+1}^2 b_{ij} X_i X_j \quad (1)$$

where Y is the dependent response variable (i.e., compressive strength of the scaffolds), b_0 is the intercept term, and b_i , b_{ii} , and b_{ij} are the measures of the effect of variable X_i , X_i^2 , and $X_i X_j$, respectively. X_i and X_j represent the independent variables. The variable $X_i X_j$ represents the first-order interaction between X_i and X_j ($i < j$).

The confidence level of 10% (P-value < 0.1) was chose for the ANOVA of the quadratic model. Also, the magnitude and the significance of the effect estimations for each of the variables and all their possible interactions were determined.

3. Results and discussion

3.1. Powder characterization

Fig. 1 shows the XRD pattern of the sphene powder sintered at 900°C. As can be seen in this figure, the major phase was sphene (JCPDS 016-02-0521). Sphene or titanite is a nesosilicate mineral with mono-clinic symmetry [14]. Various phases were formed during calcination of the sphene precursor powders which was confirmed by STA. Fig. 2 shows the DTA–TG curve of a powder sample after 1 h of milling. At first, calcium titanate appeared as the major phase along with CaO and TiO₂ around 800°C.

On further calcination at higher temperatures (900°C), CaTiO₃, CaO, and TiO₂ appeared to react with SiO₂ to form CaTiSiO₅. In both cases an exothermic peak was apparent in DTA around 800°C and 900°C for crystallization of CaTiO₃ and CaTiSiO₅ (sphene), respectively. The TG curve shows that the adsorbed water molecules and organic materials were eliminated at temperatures higher than 600 °C. The weight loss in this region was approximately 20%. Fig. 3 shows the TEM image of the sphene powder. The crystallite size of the powder is below 100 nm with highly agglomerated and irregular shapes.

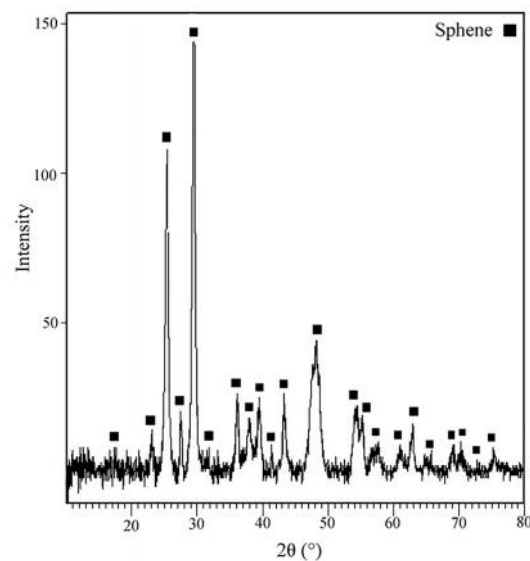


Fig. 1. X-ray diffraction pattern of the sphene powder.

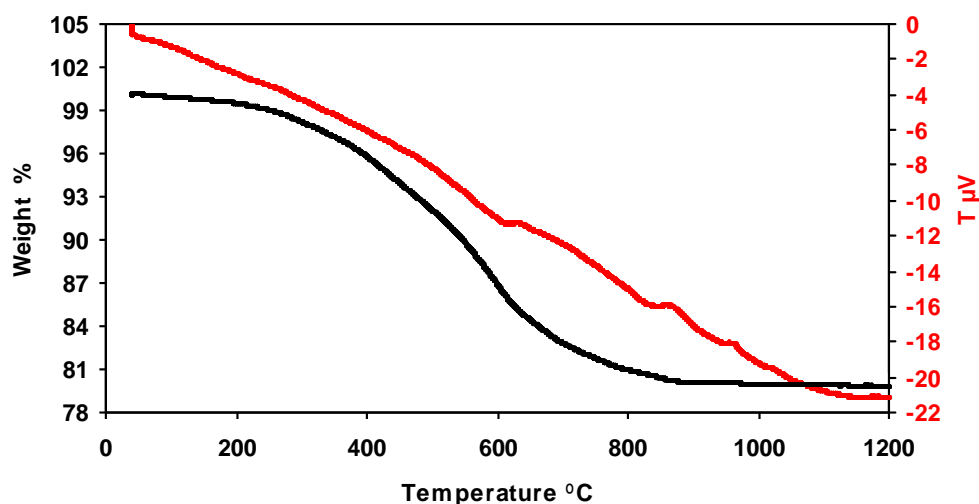


Fig. 2. Simultaneous thermal analysis curve of the sphene powder after 1 h of milling.

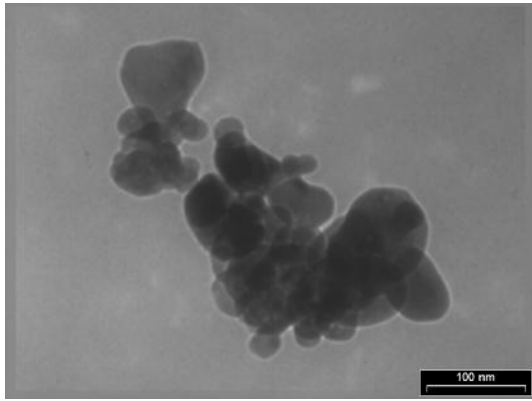


Fig. 3. TEM image of the sphene powder.

3.2. Model fitting

The values for the experimental design parameters and the response are presented in Table 2. With the help of statistical analysis, a polynomial regression model equation based on un-coded coefficients that fit 97.54% of the tolerances in the data is presented in Eq. (2):

$$\begin{aligned} \text{Compressive strength} \approx & 17.29 - 0.487(\%V) \\ & - 0.045(d) + 0.005(\%V).(d) \\ & + 0.0001(d).(d) - 6 \times 10^{-5}(\%V).(d) \end{aligned} \quad (2)$$

The low P-value of regression ($P < 0.001$), as well as the insignificance of the lack of fit ($P > 0.1$) indicate that the proposed model is suitable (Table 3).

Moreover, the predicted values for the compressive strength (from Eq. (2)) are plotted versus those obtained experimentally (Table 2) and shown in Fig. 4, which indicates the appropriate linear distribution and the adequacy of the model. (For compressive strength and stress-strain curves see the supplementary information.)

3.3. Effects of particles size and %V porogen

As shown in Fig. 5a, at low %V of porogen, decreasing the particle size (in the range of 100–300 μm) leads to an increase in the compressive strength of the sphene scaffolds. At a high level of particle diameter values, the compressive strength of the prepared scaffolds decreased because of the increase in the %V of porogen (in the range of 20%–50%). The contour plots for the compressive strength with respect to the %V porogen and particle diameter are shown in Fig. 5b. Mechanical properties of the sphene scaffolds are significantly dependent on the particle size and the amount of the used porogen. Optimization of the levels of the two factors to obtain maximum compressive strength was carried out using Eq. (2). This exercise predicted that the maximum value of the compressive strength can be obtained under the following conditions: %V < 25% and $d < 250\mu\text{m}$.

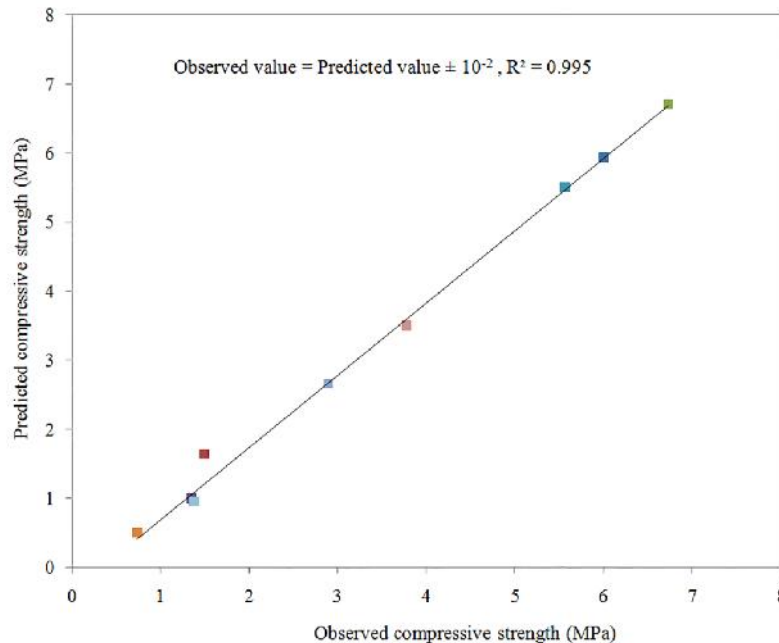


Fig. 4. Observed compressive strength versus experimentally obtained compressive strength of the manufactured sphene scaffolds.

Table 3. The ANOVA Table.

	Degrees of freedom	Sum of squares	Mean squares	F-value	P-value
Model	5	48.58	9.716	39.59	0.001
Residual	5	1.227	0.245		
Lack of fit	3	1.227	0.409	4089	0.000
Pure error	2	0.000	0.0001		
R ²	97.54				

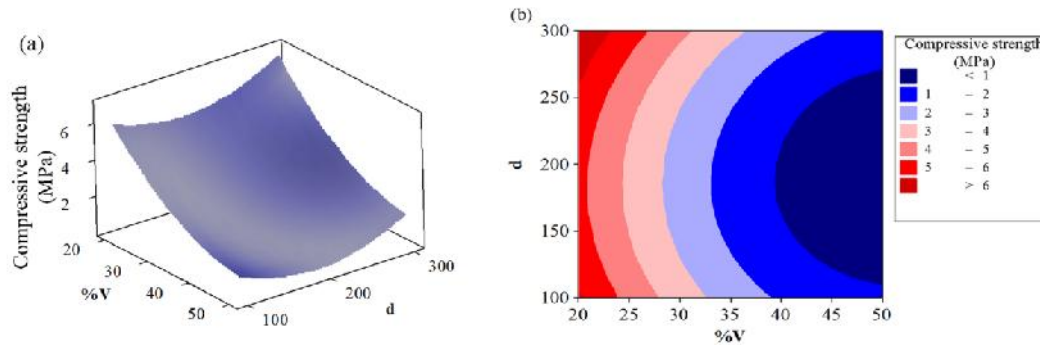


Fig. 5. The surface plot (a) and contour plot for the compressive strength (MPa) with respect to the particle size (d) and the %V porogen (%V).

Mechanical behavior of a scaffold is highly dependent on the number and size of the porosities in the structure. The use of porogen in the synthesis procedure can change the porosity value of the final scaffold; thus, the compressive strength of the sphere scaffolds varied from 1 MPa to 7 MPa when the %V of porogen was changed. This result is consistent with those reported in previous studies [15-17]. This result can be further confirmed by a close observation of Fig. 5b.

A region exists where the compressive strength is higher than 6, the particle diameter = 250 μm to 300 μm, and the %V porogen = 20% to 25%. Employing these optimal regions seems to be more facile and better from an experimental perspective because it allows using a range of factors for obtaining the desired mechanical properties of the sphere scaffolds. SEM images of the prepared sphere scaffold under optimum condition are depicted in Fig. 6.

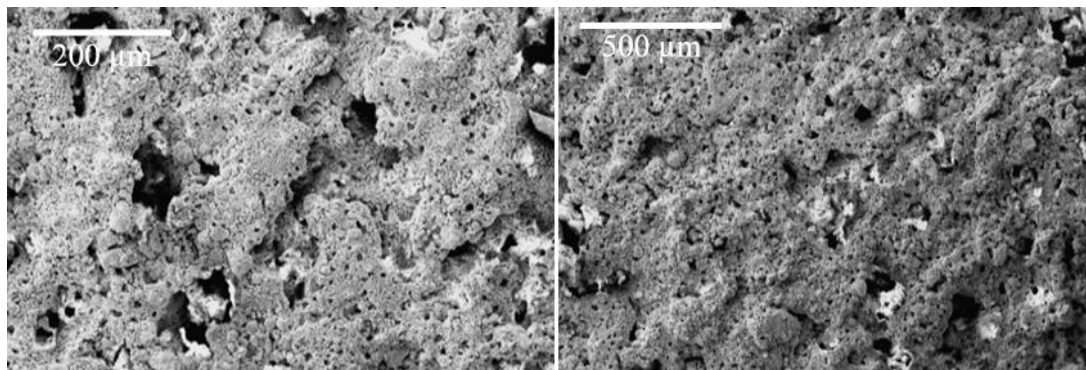


Fig. 6. SEM images of the produced sphere scaffold with two different magnifications.

4. Conclusion

Sphere powder was successfully synthesized and its scaffolds were manufactured. The effect

of particle size and %V porogen (citric acid) on the mechanical behavior of the sphere scaffolds was studied. RSM was successfully performed

to optimize the compressive strength of the sphere scaffolds. Under optimum conditions (%V porogen 25% and particle size 250 μm), the sphere scaffolds with a compressive strength as high as 7 MPa were fabricated.

Acknowledgements

This study was supported by Materials and Energy Research Center (MERC) under the grant number 721391011.

References

- [1] J. Panti, A. Kremenovi, A. Došen, M. Prekajski, N. Stankovi, Z. Bašarevi, B. Matovi, "Influence of mechanical activation on sphere based ceramic material synthesis", *Ceram. Int.*, Vol. 39, No. 1, 2013, pp. 483-488.
- [2] D. Clarke, "Ceramic materials for the immobilization of nuclear waste", *Annu. Rev. Mater. Sci.*, Vol. 13, No. 1, 1983, pp. 191-218.
- [3] Y. Teng, L. Wu, X. Ren, Y. Li, S. Wang, "Synthesis and chemical durability of U-doped sphere ceramics", *J. Nucl. Mater.*, Vol. 444, No. 1, 2014, pp. 270-273.
- [4] T. S. Lyubenova, F. Matteucci, A. Costa, M. Dondi, J. Carda, "Ceramic pigments with sphere structure obtained by both spray-and freeze-drying techniques", *Powder. Technol.*, Vol. 193, No. 1, 2009, pp. 1-5.
- [5] C. T. Wu, Y. Ramaswamy, D. Gale, W.R. Yang, K.Q. Xiao, L.C. Zhang, Y.B. Yin, H. Zreiqat, "Novel sphere coatings on Ti-6Al-4V for orthopedic implants using sol-gel method", *Acta. Biomater.*, Vol. 4, No. 3, 2008, pp. 569-576.
- [6] C. Wu, Y. Ramaswamy, A. Soeparto, H. Zreiqat, "Incorporation of titanium into calcium silicate improved their chemical stability and biological properties", *J. Biomed. Mater. Res. Part A.*, Vol. 86, No. 2, 2008, pp. 402-410.
- [7] Y. Ramaswamy, C. Wu, C. R. Dunstan, B. Hewson, T. Eindorf, G. I. Anderson, H. Zreiqat, "Sphere ceramics for orthopedic coating applications: An in vitro and in vivo study", *Acta. Biomater.*, Vol. 5, No. 8, 2009, pp. 3192-3204.
- [8] C. Wu, Y. Ramaswamy, X. Liu, G. Wang, H. Zreiqat, "Plasma-sprayed CaTiSiO₅ ceramic coating on Ti-6Al-4V with excellent bonding strength, stability and cellular bioactivity", *J. R. Soc. Interface.*, Vol. 6, No. 31, 2009, pp. 159-168.
- [9] M. Fathi, E. M. Zahrani, "Mechanical alloying synthesis and bioactivity evaluation of nanocrystalline fluoridated hydroxyapatite", *J. Cryst. Growth.*, Vol. 311, No. 5, 2009, pp. 1392-1403.
- [10] S. H. Park, H. J. Kim, J. I. Cho, "Optimal central composite designs for fitting second order response surface linear regression models", in *Response Surface Linear Regression Models*, Physica-Verlag HD, Heidelberg, 2008, pp. 323-329.
- [11] A. Amirjani, M. Bagheri, M. Heydari, S. Hesaraki, "Label-free surface plasmon resonance detection of hydrogen peroxide; a bio-inspired approach", *Sens. Actuators. B.*, Vol. 227, 2016, pp. 373-382.
- [12] A. Amirjani, P. Marashi, D. H. Fatmehsari, "Effect of AgNO₃ addition rate on aspect ratio of CuCl₂-mediated synthesized silver nanowires using response surface methodology", *Colloids. Surf., A.*, Vol. 444, 2014, pp. 33-39.
- [13] A. Amirjani, P. Marashi, D. H. Fatmehsari, "Interactive effect of agitation rate and oxidative etching on growth mechanisms of silver nanowires during polyol process", *J. Exp. Nanosci.*, Vol. 10, 2015, pp. 1387-1400.
- [14] E. S. Dana, *Manual of Mineralogy*, 17th ed., John Wiley & Sons, Inc., 1959, pp. 412-413.
- [15] M. J. Mondrinos, R. Dembzyński, L. Lu, V.K. Byrapogu, D.M. Wootton, P.I. Lelkes, J. Zhou, "Porogen-based solid freeform fabrication of polycaprolactone-calcium phosphate scaffolds for tissue engineering", *Biomater.*, Vol. 27, No. 25, 2006, pp. 4399-4408.
- [16] I. Zein, D. W. Hutmacher, K. C. Tan, S. H. Teoh, "Fused deposition modeling of novel scaffold architectures for tissue engineering applications", *Biomater.*, Vol. 23, No. 4, 2002, pp. 1169-1185.
- [17] J. M. Williams, A. Adewunmi, R. M. Schek, C.L. Flanagan, P. H. Krebsbach, S. E. Feinberg, S. J. Hollister, S. Das, "Bone tissue engineering using polycaprolactone scaffolds fabricated via selective laser sintering", *Biomater.*, Vol. 26, No. 23, 2005, pp. 4817-4827.